Fibrous Complexes of Deoxyribonucleic Acid with Certain Globular Proteins. Role of Divalent Metal Ions in the Organization of Nucleoprotein Structures*

David Kabat†

ABSTRACT: Divalent metal ions have a profound influence on the structures of many natural nucleoproteins, including ribosomes and chromosomes; however the proteins comprising these substances are heterogeneous. A study was therefore made of the effects of divalent metal ions on mixtures of deoxyribonucleic acid (DNA) with homogeneous globular proteins. The most basic of the chicken hemoglobins complexes with DNA in the presence of Mg^{2+}, Ca^{2+}, or Mn^{2+} to form insoluble fibers. Polarization and electron microscopic observations establish that the DNA molecules are oriented parallel to the fiber axis. Fibrous horse heart cytochrome *c*–DNA complexes, structurally similar to the hemoglobin–DNA complexes, also are formed only in the presence of divalent cations. Polarized visible absorption spectra of the hemoglobin–DNA and cytochrome *c*–DNA fibers were used to determine orientation of the hemoproteins relative to the fiber axes. As controls, polarized spectra of monoclinic crystals of horse methemoglobin, oxyhemoglobin, and methemoglobin azide and also of tetragonal crystals of horse heart ferricytochrome *c* were obtained. The chicken hemoglobin molecules in the nucleoprotein fibers do not appear to be strongly oriented with respect to the fiber axis. However in the horse heart cytochrome *c*–DNA fibers, the heme normals are oriented at 60° to the fiber axis. With both hemoproteins, binding to DNA does not measurably alter the visible spectrum, indicating that gross changes of polypeptide folding do not accompany the interactions. A mechanism is proposed to explain the stabilization of the tightly packed fiber structures by divalent metal ions; it is argued that this mechanism might be operative also in determining ribosome and chromosome structures.

The packing of nucleic acid molecules in viruses, ribosomes, chromosomes, and sperms involves associations of the nucleic acid with protein molecules. Although little is known concerning the organization of nucleic acids in such structures, this subject is of obvious importance to understanding the biological functioning of these molecules. Interest in this area is heightened by recent studies of hetero- and euchromatins (Littau *et al.*, 1964) and of the phenomenon of "puffing" in dipteran polytene chromosomes (Kroeger and Lezzi, 1966) which suggest that the tightness of packing of chromosomal DNA chains might be an important factor in the regulation of genetic activity.

There are many instances in which divalent cations exert a profound influence on nucleoprotein structure; this has been most thoroughly studied in the cases of ribosomes (Goldberg, 1966; Gavrilova *et al.*, 1966), chromosomes (Mazia, 1954; Somers *et al.*, 1963), and sea urchin sperms (Mazia, 1954; Solari, 1965). In all cases the effect appears similar in that tight packing of the nucleoprotein occurs in the presence of divalent cations, whereas swelling of the nucleoprotein occurs upon divalent cation removal; this raises the possibility that a common mechanism might be involved. Unfortunately, the naturally occurring nucleoproteins generally contain heterogeneous protein components; this has greatly complicated analysis of the protein–nucleic acid interactions.

It is the purpose of this paper to describe the divalent cation-dependent formation of the tightly packed fibrous complexes chicken Hb–DNA[1] and horse heart Cy *c*–DNA. A role for divalent cations in these fibers, possibly relevant to the general involvement of divalent cations in nucleoprotein structures, is suggested to account for the observations. It is further shown that the DNA double helices are oriented parallel to the nucleoprotein fiber axes and that the Cy *c* molecules (possibly also the Hb molecules) are strongly oriented with respect to the fiber direction.

Materials and Methods

Protein Preparation. Blood of normal, adult, White Leghorn chickens was obtained by heart puncture with heparin as anticoagulant, and the cells were washed thoroughly with 0.13 M NaCl, 0.005 M KCl, and 0.0075 M $MgCl_2$. The buffy coat of leukocytes was

* From the Division of Biology, California Institute o Technology, Pasadena, California. *Received June 23, 1967* Supported by the U. S. Public Health Service Grant GM-11726 and by a predoctoral fellowship from the National Science Foundation.

† Present address: Department of Biology, Massachusetts Institute of Technology, Cambridge, Mass.

[1] Abbreviations used: Hb, hemoglobin; Cy *c*, cytochrome *c*.

removed. Hemolysis was accomplished by suspending one volume of packed cells in two volumes of distilled water at 2° for 30 min. The hemolysates were centrifuged at 105,000*g* for 3 hr to sediment the ribosomes. The resulting Hb solutions were dialyzed exhaustively *vs.* 0.01 SSC (0.0015 M NaCl–0.00015 M sodium citrate, pH 6.9), and were then stored in a N_2 atmosphere in Thunberg tubes. Fresh heparinized horse blood was obtained from Dr. W. D. Ommert (Monrovia, Calif.). The washing of horse erythrocytes and preparation of Hb were the same as for the chicken erythrocytes.

Chromatographic purification of chicken hemoglobins on Amberlite IRC-50 columns (Mallinckrodt CG-50, 200–400 mesh, 10 mequiv/g) was done by an adaptation of the method of Van der Helm and Huisman (1958). Citrate buffer of ionic strength equal to 0.15 M (Huisman and Prins, 1955) was adjusted to lower ionic strength by dilution and to higher ionic strength by addition of solid NaCl. Hemoglobins were eluted by stepwise increments of ionic strength. Larger columns were employed by using proportionately larger volumes of eluent. Fractionated hemoglobins were precipitated with 80% $(NH_4)_2SO_4$, resuspended and dialyzed *vs.* 0.01 SSC, and then stored under N_2 in Thunberg tubes.

Oxidation to give methemoglobin was done by dialysis of the Hb against 0.001 M $K_3Fe(CN)_6$, followed by dialysis *vs.* 0.01 SSC. Methemoglobin azide was prepared by adding a few grains of NaN_3 to solutions of methemoglobin.

Horse heart ferricytochrome *c* (type III) was purchased from Sigma Chemical Co. Ferrocytochrome *c* was prepared by adding a few grains of $Na_2S_2O_4$ to solutions of the oxidized protein.

Preparation and Composition Analysis of Nucleoprotein Fibers. Highly polymerized calf thymus DNA (type I, Sigma Chemical Co.) was dissolved and thoroughly dialyzed with 0.01 SSC. Its sedimentation coefficient, determined using a Spinco Model E analytical ultracentrifuge with ultraviolet optics, was 18.3 S in 0.7 M NaCl, corresponding therefore to a molecular weight of approximately 5.6×10^6 (Burgi and Hershey, 1963). The DNA exhibited the melting profile expected for native double-helical material (Marushige and Bonner, 1966). In one experiment, this DNA was sonicated by the method of Doty *et al.* (1958), resulting in material with sedimentation coefficient of 5.6 S, and therefore having a molecular weight of approximately 3×10^5 (Doty *et al.*, 1958). Denatured DNA was produced by heating dialyzed and highly polymerized DNA (100 μg/ml) at 100° for 10 min followed by rapid cooling in ice. Human liver 28S rRNA was a gift of Drs. G. Attardi and F. Amaldi.

A soluble complex between Cy *c* and DNA was prepared as described by Olivera (1966). Solutions of Cy *c* and DNA in 1 M NaCl were mixed in different proportions and were then thoroughly dialyzed (good agitation is necessary) *vs.* 2.5×10^{-4} M EDTA (pH 6.8). Some factors involved in the preparation of chicken Hb–DNA and horse heart Cy *c*–DNA fibers are described below (see Results). Unless otherwise mentioned, nucleoprotein fibers for structural studies were formed by adding 0.05 ml of protein solution (25 mg/ml in 0.01 SSC) to 1.5-ml solutions of DNA (0.10 mg/ml in 0.002 M NaCl–0.002 M sodium cacodylate–0.0012 M $MgCl_2$, pH 6.5). Such fibers reproducibly had the mass ratios Hb:DNA equal to 3.4 (1 Hb:64 P) or Cy *c*:DNA equal to 3.8 (1 Cy *c*:20 P).

Occasionally, nucleoprotein fibers were disrupted by treatment with DNase. Fiber suspensions in 0.01 SSC at the concentration of 100 μg/ml of DNA were digested with 10 μg/ml of DNase (Worthington) for 20 min at 37° after addition of 0.0024 M $MgCl_2$.

Generally, nucleoprotein fibers were suspended in 1.0 M NaCl for 15 hr at 4°; this treatment caused slow solubilization of the fibers. In the case of Cy *c*, absorbance of the solutions was measured following reduction of the iron with $Na_2S_2O_4$. Absorbance of solutions containing methemoglobin was measured at 260 mμ before conversion to cyanmethemoglobin (by the addition of 10-μl/ml solution of 0.08 M KCN–0.06 M $K_3Fe(CN)_6$). Concentrations of hemoprotein and of DNA were determined spectrophotometrically using the following molar absorptivities: calf thymus DNA at 260 mμ (6.40×10^3 l./mole of DNA P), hemoglobin at 260 mμ (4.03×10^4 l./mole of iron), oxyhemoglobin at 414 mμ (15.7×10^4 l./mole of iron) or at 542 mμ (1.49×10^4 l./mole of iron), cyanmethemoglobin at 540 mμ (1.15×10^4 l./mole of iron), and ferrocytochrome *c* at 521 mμ (1.59×10^4 l./mole of iron) (Margoliash and Frohwirt, 1959) and at 260 mμ (3.62×10^4 l./mole of iron). In all cases, absorbance at 260 mμ owing to DNA was taken to be the measured absorbance minus the absorbance owing to protein. The above molar absorptivities were calculated from measured values of absorbance per milligram using the molecular weights 6.8×10^4 for chicken Hb (four irons per molecule) (Saha, 1964) and 1.23×10^4 for horse heart Cy *c* (one iron per molecule) (Margoliash and Frohwirt, 1959). The average molecular weight of a DNA nucleotide was taken to be 320. Water content of the nucleoprotein fibers was measured as the weight change when the fibers were dried in an oven at 100° for 45 min.

Polarization Microscopy. Nucleoprotein fibers were withdrawn from the mother liquor with forceps and pressed gently against glass to blot away adhering solution. After allowing the fibers to dry slightly in air (5 min at 25° at about 35% relative humidity), the fibers were placed onto clean glass slides, covered with immersion oil (n_D 1.515; Cargille Laboratories, Inc.), and observed in a Carl Zeiss (Jena) polarizing microscope with a tungsten arc light source and transformer (Model 393) purchased from Spencer Lens Co. (Buffalo, N. Y.). Nucleoprotein fibers handled in this manner contained reproducibly 35–50% water by weight. The birefringence of colored materials is complicated owing to light absorption by the sample (Perutz and Mitchison, 1950); consequently, regions of the fibers so thin as to appear colorless were selected for analysis. Birefringence was quantitatively measured by compensator methods (Stoves, 1957).

Electron Microscopy. In order to prepare nucleoprotein fibers for electron microscopic observation, it was necessary to break the fibers into small pieces. However, in solutions containing divalent metal ions, the fibers associate and dispersion is not possible. Consequently, fibers were dispersed by vigorous agitation in low ionic strength solution lacking divalent cation (0.01 SSC). Dispersed nucleoprotein was placed onto 300 mesh copper grids previously covered with parlodion film and excess liquid was drawn off. Staining of grids was accomplished by floating them face-down for 15 min on aqueous solutions either of 4% phosphotungstic acid–0.4% sucrose (pH 6.5) or else on 2% uranyl acetate. Excess stain was drawn off by touching the edge of the grids with filter paper. Some grids were shadowed with Pt–Pd metal at an angle of 30°. Preparations were viewed with a Phillips 200 electron microscope.

Protein Crystals. There has been confusion in the literature concerning the appearance and absorption of light by horse hemoglobin crystals (Murayama *et al.*, 1965). Figure 1 shows a photograph of monoclinic horse methemoglobin crystals (space group C2). Crystals were grown by dialysis against 50% $(NH_4)_2SO_4$ or 2.4 M K_2HPO_4 (pH 7.0) (Perutz, 1947). Such crystals are flat plates in the [001] plane, the only other faces being commonly well developed are the [110] and [1$\bar{1}$0] faces. Unit cell dimensions are a = 109 A, b = 63.2 A, c = 54.4 A, and β = 111°. The accompanying diagram shows the orientation of the unit cell b axis relative to the crystal faces and also the orientation of the heme groups in the crystal as given by Ingram *et al.* (1956). A principal direction of refraction of these crystals is the b axis, as is generally true for monoclinic crystals (Wood, 1964).

Tetragonal crystals (space group $P4_1$) of horse heart ferricytochrome c were a gift of Dr. R. E. Dickerson. These crystals have been described (Margoliash and Schejter, 1966). The unit cell dimensions are a = 58.45 A, b = 58.45 A, c = 42.34 A, and β = 90°; there are four molecules in the unit cell related by a fourfold screw axis parallel to the c direction which is also the major axis of the needlelike crystals. The predominant crystal faces parallel to c are the [100] and [010] planes, which are optically equivalent due to crystal symmetry. The c axis of tetragonal crystals is the optic axis (Wood, 1964).

Measurement of Polarized Absorption Spectra. The absorption spectra of protein crystals and nucleoprotein fibers were obtained using a Cary Model 15 recording spectrophotometer with a microscope attachment borrowed by Drs. M. Delbrück and K. Zankel from Applied Physics Corp. The microscope attachment replaced the usual sample compartment of the spectrophotometer. The sample beam of the spectrophotometer was focused with a 20×, 0.5 N.A. microscope objective to form a 10 × 10 μ image at the microscope stage. Specimens analyzed in these experiments were always at least several times larger than this image. The light was collected by a 90×, 1.30 N.A., oil immersion objective. Viewing was accomplished by means of a

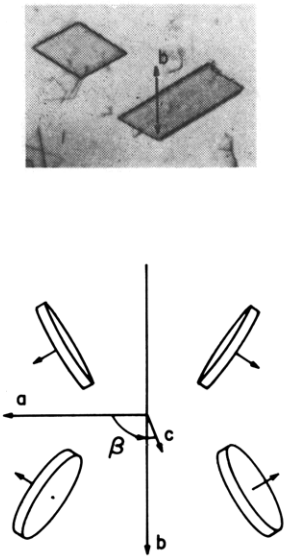

FIGURE 1: Photograph of horse hemoglobin crystals and arrangement of the heme groups. Positions of the heme groups were taken from Ingram *et al.* (1956). The upper and lower disks represent, respectively, α- and β-chain hemes. The angles between the heme normals and b (the twofold rotation axis) are 58 and 57° for the α- and β-chain hemes, respectively. The b axis bisects the obtuse, 120°, angle of the crystals.

removable mirror and auxiliary ocular which contained reference lines drawn parallel and perpendicular to the polarizer directions. Metal disks with holes were used in the reference beam as neutral density filters to balance losses in the microscope optics. A base line was obtained for each spectral curve by moving the specimen out of the beam and sending the beam through a section of the slide adjacent to the specimen; the absorbance was taken as the difference between these curves. The monochromator slits were held fixed at 0.3 mm, resulting in a spectral band width of 2.5–8.5 mμ in the wavelength range from 400 to 600 mμ. The apparatus was capable of measuring absorbance to 0.003. Calibration and adjustment of the instrument were performed by K. Zankel and P. Burke.

The protein crystals and nucleoprotein fibers, suspended in mother liquor, were placed on microscope slides and covered with coverslips which were spaced from the slides with dabs of stopcock grease. This served to immobilize the crystals, without crushing them. Immersion oil was placed between the coverslip and the collecting objective. The specimens could be positioned by the usual methods on a rotating microscope stage. The specimen selected for observation was then rotated so that its principal direction of refraction was accurately aligned parallel to one of the reference lines marked on the viewing ocular.

The polarizer used was a piece of polaroid mounted in clear glass and marked so as to indicate the directions parallel and perpendicular to the electric vector of the

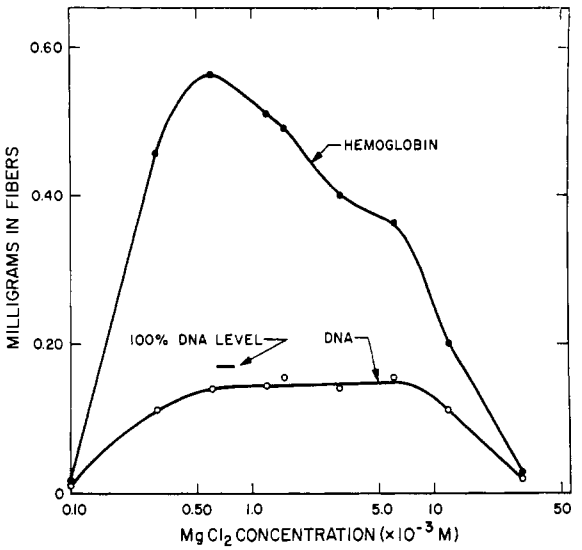

FIGURE 2: Composition of Hb–DNA fibers as a function of $MgCl_2$ concentration. To 1.5-ml aliquots of DNA (0.17 mg) in 0.002 M Tris buffer (pH 7.0) were added varying amounts of 1.2 M $MgCl_2$ at 2°. Chicken Hb (0.1 ml containing 2.5 mg of Hb) was added to each aliquot and the tubes were immediately centrifuged at 2000*g* for 2 min to sediment the fibers. Fiber composition was analyzed as described in Materials and Methods.

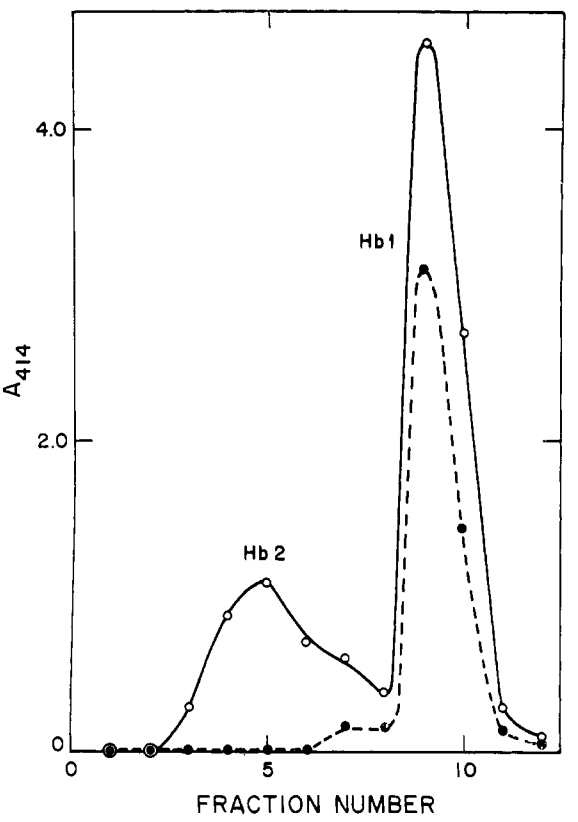

FIGURE 3: Anion-exchange chromatography of chicken hemoglobins. Amberlite 1RC-50 columns measured 1 × 4 cm, and fractions contained 1.0 ml of eluate. The elution employed stepwise increment of ionic strength as follows (fraction numbers indicated in parentheses): 0.075 (1), 0.15 (2), 0.20 (3–8), and 0.40 M (9–13). (—○—) Total cell Hb; (- - -●- - -) Hb extracted from Hb–DNA fibers (Hb:DNA mass ratio, 3.4) by DNase treatment (see Materials and Methods).

transmitted light. For this polarizer, the out-of-plane component was a maximum of $^1/_{160}$ of the in-plane intensity (measured using two equivalent polaroids on top of each other and assuming that the intensity transmitted when the polarizers are crossed at 90° is at least twice the out-of-plane intensity passed by either filter). It is readily calculated that for a specimen with a dichroic ratio of 2.0 and a measured absorbance of 1.0 in the direction of strong absorption, the error in the measured absorbance will consequently be less than ±0.01 absorbance unit (Stewart and Davidson, 1963). The polarizer was placed in the sample beam just above the 90× collecting objective and was taped onto a metal platform containing an aperture through which the light passed. By aligning the reference marking on the polarizer with markings on the metal bar, the polarizer could be accurately positioned either parallel or perpendicular to the principal directions of the specimen. Such polarized absorption spectra were reproducible to within a few per cent (*ca.* ±4%).

Analysis of Polarized Absorption Spectra. Circularly polarized light shone through a birefringent crystal face will be resolved into two mutually perpendicular plane polarized beams. The polarization directions (x and y), called here the "principal axes of refraction," are generally fixed by crystal symmetry (Wood, 1964). Absorbance of light polarized in each of these directions is measured, the ratio $A_x:A_y$ being termed the dichroic ratio, or D. Absorbance in either direction is proportional to the square of the direction cosine between the polarization direction and the direction of the transition moment for allowed electronic excitation of the chromophore. As discussed below (see Discussion), the heme group can, as a first approximation, be considered an "ideal two-dimensional absorber" between 470 and 600 mμ. According to this approximation, the absorption in this region is interpreted as being due to two degenerate (*i.e.*, equal energy) and perpendicularly polarized π–π^* transitions lying in the heme plane. This approximation is similar to assuming that the heme group has square symmetry, all four pyrrole rings being electronically equivalent (Platt, 1956).

The absorption of polarized light by monoclinic horse methemoglobin crystals has previously been shown to be consistent with the idea that the heme groups act as ideal two-dimensional absorbers (Ingram *et al.*, 1956). For such absorption, the dichroic ratio ($A_{\parallel b}:A_{\perp b}$) for light shone through [001] will agree closely with the equation $D = \tan^2\theta$, where θ is the mean angle between the heme normals and the b axis

TABLE I: Independence of Fiber Composition on Hemoglobin Concentration.[a]

Sample	mg of Hb Added	mg of Hb in Fibers	mg of DNA in Fibers	Mass Ratio in Fibers (Hb:DNA)
1	0.13	0.097	0.041	2.4
2	0.27	0.20	0.076	2.6
3	0.81	0.41	0.15	2.65
4	1.20	0.42	0.16	2.6
5	1.91	0.43	0.17	2.6
6	2.76	0.42	0.15	2.7

[a] To 1.5-ml aliquots of DNA (0.18 mg) in 0.002 M Tris (pH 7.0) containing 0.0030 M $MgCl_2$ were added 0.1-ml dilutions of Hb in the same buffer at 2°. Fibers were sedimented at 2000*g* for 5 min and fiber composition was analyzed as described in Materials and Methods.

(in these crystals the α-chain heme normals lie at 58° and the β-chain heme normals at 57° with respect to *b*).

If the heme groups in the tetragonal horse ferricytochrome *c* crystals are simple two-dimensional absorbers as just defined, then the dichroic ratio ($A_{\parallel c}:A_{\perp c}$) for light shone through [100] or [010] will be given by $D = (2\sin^2\theta/(1 + \cos^2\theta))$, where θ is the angle between any heme normal and *c* (the fourfold rotation axis).

In the nucleoprotein fibers, the fiber axis (also a principal axis of refraction) can probably be considered (from the standpoint of the protein molecules) an axis of rotational symmetry; this assumption is based on the helical nature of DNA and is described below (see Discussion). The calculation of light absorption by heme groups located on such an axis is very similar to that just described for the *c* axis of Cy *c* crystals. That is, for ideal two-dimensional absorbers the dichroic ratio ($A_{\parallel \text{fiber}}:A_{\perp \text{fiber}}$) is given by $D = (2\sin^2\theta/(1 + \cos^2\theta))$, where θ is the angle between the heme normal and the fiber axis. For Cy *c*–DNA fibers, the dichroism for ideal absorption will be given by the latter equation assuming that the Cy *c* molecules are all similarly oriented with respect to the fiber axis. On the other hand, the interpretation of absorption by Hb–DNA fibers is further complicated by the fact that the protein contains four hemes.

Results

Formation of Chicken Hemoglobin–DNA Complexes. When chicken Hb is added to solutions of highly polymerized DNA in low ionic strength buffers (pH 7.0) containing divalent cations (Mg^{2+}, Ca^{2+}, or Mn^{2+}), large red fibers rapidly form; these fibers may be sedimented by low-speed centrifugation (2000*g* for 2 min) or withdrawn on forceps. In the absence of added divalent cations, mixtures of Hb and DNA become turbid upon prolonged standing, but no fibers appear; nonfibrous nucleoprotein can be sedimented from these turbid solutions (*e.g.*, 10,000*g* for 10 min). In all buffer systems examined, the Hb:DNA mass ratio in the nonfibrous nucleoprotein is lower than the mass ratio in the fibers formed at low Mg^{2+} levels (*e.g.*, 3×10^{-4} M $MgCl_2$). Apparently, the divalent cation-induced change of nucleoprotein structure is associated with an increased level of Hb binding.

Some characteristics of the fiber formation are presented in Figure 2 which shows the DNA and Hb content of the fibers at varying levels of added $MgCl_2$. The Hb:DNA mass ratio in the fibers declines as the $MgCl_2$ concentration is increased; at concentrations above approximately 0.01–0.02 M $MgCl_2$, no fibers form.

To solutions containing constant $MgCl_2$ and DNA concentrations, various amounts of Hb were added with rapid mixing, and the fibers were analyzed for Hb and DNA composition (Table I). The Hb:DNA ratio in the fibers remains constant over a wide range of input Hb; in the conditions used (0.002 M Tris–0.003 M $MgCl_2$, pH 7.0), the mass ratio is approximately 2.6. As also seen in Table I, when Hb is added in amounts insufficient to fully complex all of the DNA, a portion of the DNA forms fibers fully covered with the Hb, whereas the Hb:DNA mass ratio in the mother liquor is relatively low (it is shown below that there is a fraction of chicken Hb (*ca.* 25%) which does not complex with DNA). These data suggest that Hb molecules bind much more strongly to the fibers than to DNA molecules in solution, implying that the binding to the fibers may be highly cooperative.

The requirement for divalent cations (Mg^{2+}, Ca^{2+}, and Mn^{2+}) is stringent in the sense that NaCl, KCl, or NH_4Cl is ineffective *at all concentrations* in stimulating Hb–DNA fiber formation. The above divalent metal ions are known to interact strongly with nucleic acids, probably binding to the negatively charged phosphate residues of the backbone (Shack and Bynum, 1959; Steiner and Beers, 1961).

Although two different kinds of Hb are present in chicken erythrocytes in the approximate ratio Hb1:Hb2 equal to 3:1 (Huisman *et al.*, 1964; Manwell *et al.*, 1963; Saha, 1964), the Hb isolated from nucleoprotein fibers consists exclusively of the more basic

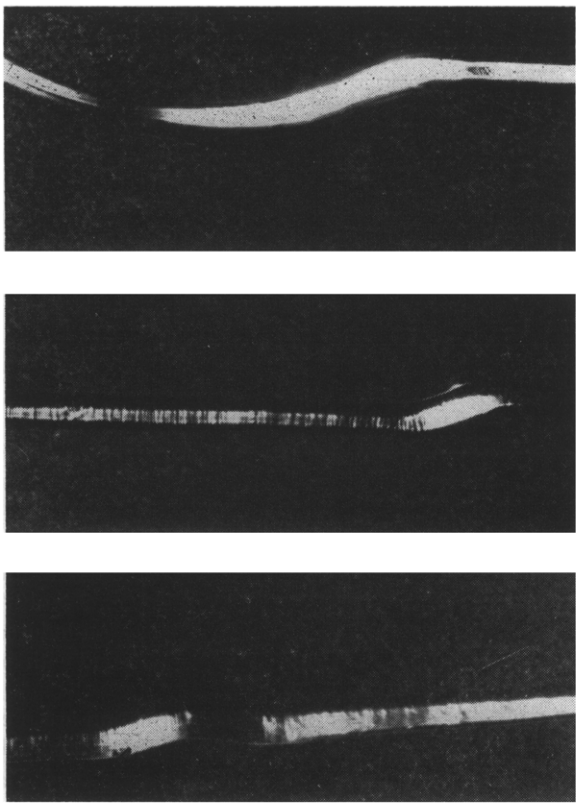

FIGURE 4: Birefringence of chicken Hb–DNA fibers. The main fiber axis is a principal direction of refraction. DNA molecules are aligned parallel to the fiber axis (see text). Occasional fibers appear to contain transverse bands which might indicate that ordered regions in a fiber are occasionally interrupted by more disordered regions or that the parallel DNA molecules occasionally bend (as in a crystal dislocation) in a new direction. That the banding is probably not an interference phenomenon is suggested by the finding that the pattern of banding does not change when colored filters are placed over the light source. The Hb:DNA mass ratio of the fibers was 3.4. Magnification is *ca.* 206×.

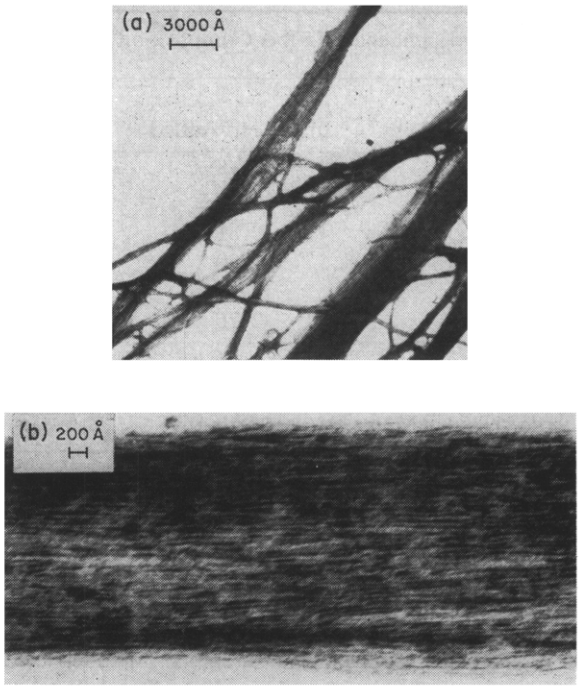

FIGURE 5: Electron micrographs of chicken Hb–DNA fibers. Nucleoprotein fibers were prepared for observation in the electron microscope as described (Materials and Methods). Uranyl acetate stained Hb–DNA. (a) About 20,000×; (b) *ca.* 109,800×.

protein, Hb1 (Figure 3). It should be mentioned that although several investigators have described heterogeneity of the Hb within the peak labeled Hb2 (Figure 3) (Matsuda and Takei, 1963; Hashimoto and Wilt, 1966), the available evidence supports the idea that Hb1 is a single protein. Chicken Hb1 is fairly basic, being isoionic at approximately pH 8.6 and having a net charge of roughly +17 at pH 7.0 as based on its amino acid composition (Saha, 1964). This is consistent with the idea that the protein may form electrostatic bonds with the negatively charged DNA phosphate groups; however possibly only a few of the positive charges on the Hb1 are involved in the interaction with DNA. In typical fibers used in this study (Hb:DNA mass ratio equal to 3.4), there is 1 Hb molecule/64 DNA phosphates. This number of Hb molecules is much too low to neutralize all of the negative charges on the DNA. Therefore, the great majority of the phosphate groups in the fibers must be combined with counterions, presumably the divalent metal ions shown to be needed for the fiber formation.

A test was made of the influence of nucleic acid structure on its association with chicken Hb. Mixtures of Hb with 28S rRNA or with sheared or thermally denatured DNA (in all cases the nucleic acid concentration was 100 μg/ml in 0.002 M Tris, pH 7.0) became immediately turbid when adjusted to 0.001 M $MgCl_2$; however no fibers formed in these solutions. Apparently, fiber formation requires native highly polymerized helical DNA, whereas divalent cation-induced aggregation of nucleoprotein occurs also with the other polynucleotides.

The observations described in this section indicate that divalent metal ions contribute strongly to the stabilization of the Hb–DNA fibers. In agreement with this conclusion, the fibers are unstable and break apart when placed in low ionic strength solutions which lack divalent metal ions (see Materials and Methods). In view of the complexity of the nucleoprotein aggregation, which presumably involves a variety of forces, no attempt was made to investigate all conceivable environmental parameters. It should be mentioned, however, that at pH values below 6.7 and in the absence of divalent cations, the nonfibrous aggregates appear more rapidly, upon mixing the Hb and DNA, than at the higher pH values described above. Furthermore,

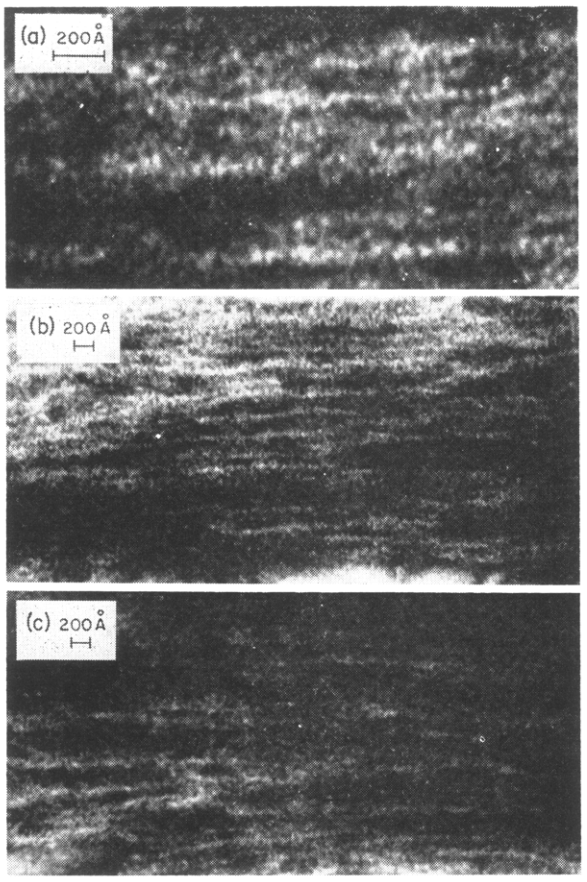

FIGURE 6: Electron micrographs of chicken Hb–DNA fibers. Phosphotungstic acid stained Hb–DNA. (a) About ×330,000; (b and c) *ca.* ×109,800.

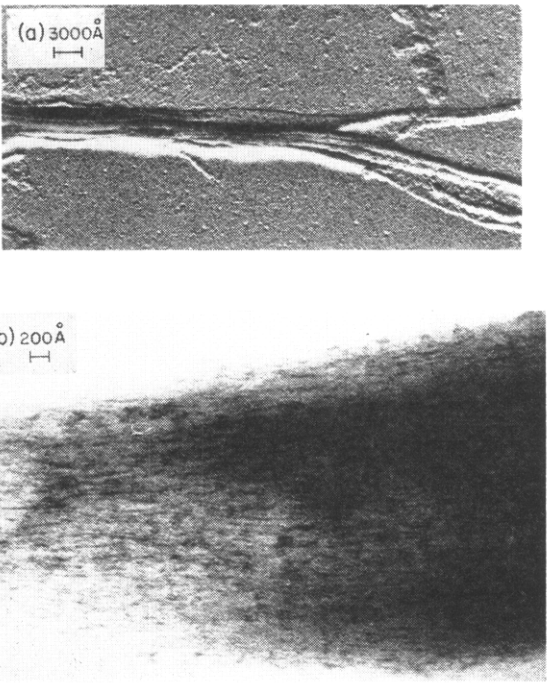

FIGURE 7: Electron micrographs of chicken Hb–DNA and horse heart Cy *c*–DNA fibers. (a) Pt–Pd shadowed Hb–DNA, *ca.* ×213,465; (b) uranyl acetate stained Cy *c*–DNA, *ca.* ×116,000.

fibers formed at the lower pH values in the presence of $MgCl_2$ are larger and are less easily broken than those formed at pH 7.0. Presumably, the protein–DNA binding is stronger at the lower pH values because the protein is more positively charged. In this context it may be mentioned that coiling of animal cell chromosomes is also stimulated both by pH decrease and by divalent cation addition (Cole, 1967).

Birefringence of Hemoglobin–DNA Fibers. Viewed in a polarization microscope, the Hb–DNA fibers appear highly birefringent (Figure 4), indicating that the refractive indices differ parallel and perpendicular to the fiber axis (these refractive indices are designated $n_{||}$ and $n_{\perp}$, respectively, the magnitude of birefringence being $n_{||} - n_{\perp}$). The strong negative briefringence of DNA fibers is intrinsic and due largely to the unsaturated purine and pyrimidine bases which lie perpendicular to the long axis of the molecules; the form birefringence of fibers is positive in sign (Maestre and Kilkson, 1965). Protein molecules have negligible intrinsic birefringence as compared with DNA; accordingly, the negative sign of birefringence in a large number of sperm heads is in agreement with the orientation of the DNA molecules (Pattri, 1932; Inoue and Sato, 1962). In the case of Hb–DNA fibers, the birefringence is negative (approximate value, −0.015 for fibers having a Hb:DNA mass ratio 3.4), implying an orientation of DNA molecules parallel to the fiber axis.

Electron Microscopy of Hemoglobin–DNA Fibers. Figures 5–7 show representative features of Hb–DNA fibers as seen in the electron microscope. Large fibers were disrupted (see Materials and Methods) in order to obtain material sufficiently small for convenient observation. The large fibers are composed of much smaller fibrillar elements running parallel to the main fiber axis (*e.g.*, Figures 5b and 6a–c). In partially disrupted fibers, branching is observed and the "cleavage" direction runs parallel to the fiber axis (*e.g.*, Figure 7a). This information is all consistent with the idea that the individual DNA molecules are oriented parallel to the fiber axis and that the lateral associations between DNA molecules are due to noncovalent linkages, presumably involving protein bridges. In this context it is of interest that fiber formation and growth can be watched in the light microscope; small fibers adhere laterally and the area of association then rapidly grows as the fibers are forcefully pulled together in a zipperlike fashion.

The uranyl acetate or phosphotungstic acid stains do not deeply penetrate the nucleoprotein fibers; rather, the stains appear to lie primarily in troughs and other irregularities on the fiber surfaces. This conclusion is based on the following information. (i) Although the fibers are rounded as seen by Pt–Pd

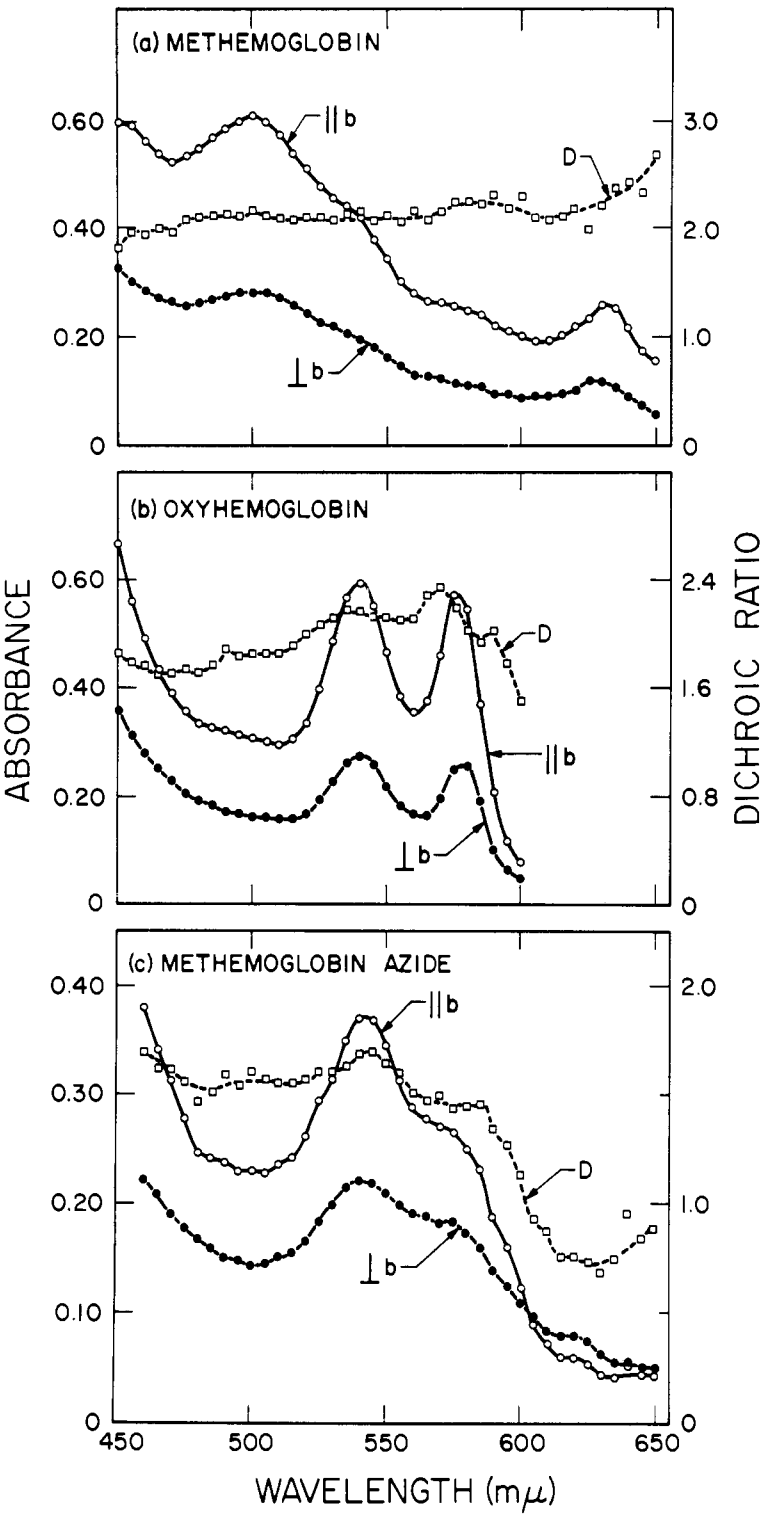

FIGURE 8: Polarized absorption spectra of horse hemoglobin crystals. Spectra were taken with light shone through the [001] plane and polarized parallel and perpendicular to the *b* axis. (a) Methemoglobin, (b) oxyhemoglobin, and (c) methemoglobin aside. (-o-o-) Electric vector parallel to *b* (||*b*). (-●-●-) Electric vector perpendicular to *b* (⊥*b*). (--□--□--) Dichroic ratio.

shadowing (Figure 7a), the staining is not systematically more intense for the larger fibers (Figure 5a). (ii) At high magnification one can see fine structure in the fibers (Figures 5b and 6a–c). If the stain deeply penetrated into the fibers, small objects would probably not be discernible. (iii) When stained grids are briefly washed with water, the stain is mostly removed, as expected if it were lying on the fiber surfaces. Consequently, the unstained fibrillar elements seen in the fibers may be identified with nucleoprotein, whereas the dark areas are probably interfibril troughs filled with stain.

At high magnification, Hb–DNA fibers stained with uranyl acetate (Figure 5b) appear very different from fibers stained with phosphotungstic acid (Figure 6a–c). The uranyl acetate stained fibers appear to be composed of parallel fibrils which measure approximately 20-A thick (Figure 5b). It seems reasonable to identify fibrils of this size with single DNA molecules. Since no hemoglobin molecules can be seen in fibers stained in this fashion, I infer that uranyl acetate solutions may extract the protein from the surface DNA.

On the other hand, the surfaces of fibers stained with phosphotungstic acid appear to contain numerous small particles (roughly 35–55 A) often arranged in rows approximately parallel to the fiber axis (Figure 6a–c). These particles are the size expected for single Hb molecules (Perutz, 1965).

Horse Heart Cytochrome c–DNA Fibers. Horse heart Cy *c* forms a soluble complex with DNA in the absence of divalent metal ions (Olivera, 1966). In the present study it was found that addition of divalent cation (Mg^{2+}, Ca^{2+}, or Mn^{2+}) to such soluble complexes results in precipitation of insoluble nucleoprotein fibers, strikingly similar in appearance to Hb–DNA fibers. Cy *c*–DNA fibers can also be formed by adding the protein to mixtures of the metal ion and DNA; fibers used in all structural studies were formed by the latter route and had a Cy *c*:DNA mass ratio of 3.8 (see Materials and Methods for fiber preparation).

Cy *c*·DNA fibers are negatively birefringent ($\Delta n = -0.026$), suggesting an alignment of DNA molecules parallel to the fiber axis. Preliminary studies with the electron microscope are in agreement with this conclusion, the fibers appearing to consist of laterally associated small fibrils (*e.g.*, Figure 7b). However particles the size expected for Cy *c* molecules (roughly 25-A globules) have not yet been clearly visualized in these fibers.

Polarized Visible Spectra of Hemoglobin–DNA Fibers. To determine the orientation of Hb molecules with respect to the nucleoprotein fiber axis, the visible absorption spectrum of the fibers was measured in polarized light. As a control, horse Hb crystals of known structure (Perutz, 1965) were investigated. Horse oxyhemoglobin, methemoglobin, and methemoglobin azide crystals are isomorphous and were all analyzed.

Figure 8 shows the polarized absorption spectra of horse Hb crystals for light passing through the [001] plane. For methemoglobin, the dichroic ratio (approximately 2.1) is nearly independent of wavelength. Previous polarized absorption studies of horse methemoglobin crystals, viewed also through [001], showed a dichroic ratio independent of wavelength and equal to 2.6 (Perutz, 1939). The findings reported here generally corroborate the results of Perutz (1939) and are in agreement with the idea that the absorption transition

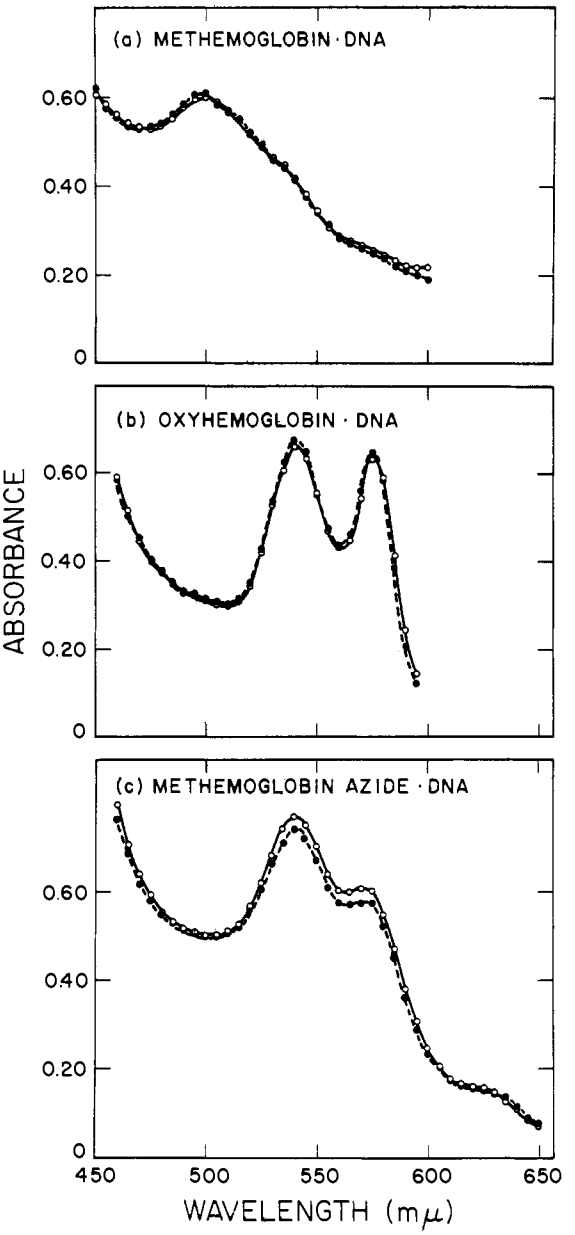

FIGURE 9: Polarized absorption spectra of chicken Hb–DNA fibers. Spectra were taken with light polarized parallel and perpendicular to the fiber axis (a principal axis of refraction). (a) Methemoglobin–DNA, (b) oxyhemoglobin–DNA, and (c) methemoglobin azide–DNA. (-o-o-) Electric vector parallel to fiber axis. (---●---●---) Electric vector perpendicular to fiber axis.

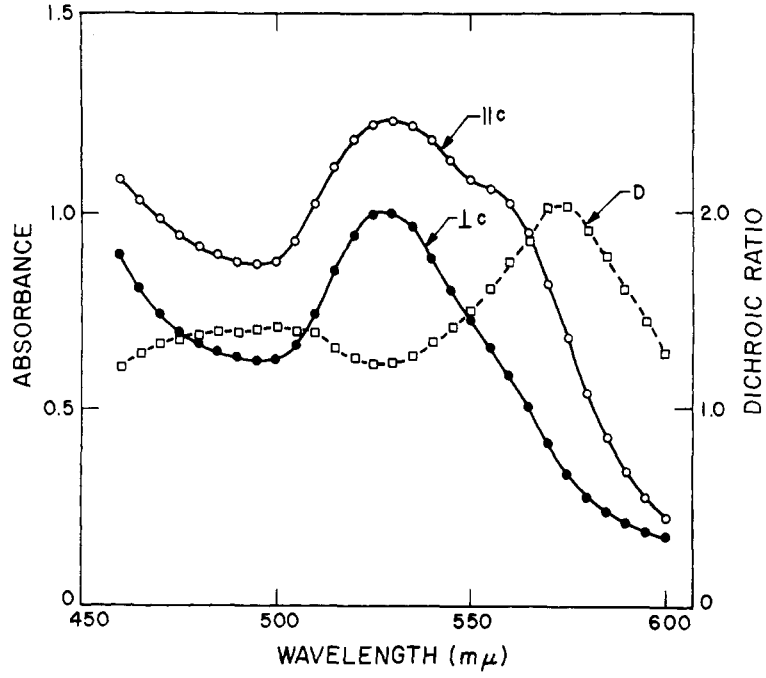

FIGURE 10: Polarized absorption spectra of horse heart ferricytochrome *c* crystals. Light was shone through [100] or [010] which are optically equivalent due to crystal symmetry. (–○–○–) Electric vector parallel to *c*. (–●–●–) Electric vector perpendicular to *c*. (---□---□---) Dichroic ratio.

moments lie in the heme planes (π–π^* transitions) and that the heme normals lie roughly in the *a* direction (see Figure 1). The fact that the methemoglobin crystal spectra are indistinguishable in shape from the methemoglobin solution spectrum, supports the reliability of the spectroscopic method employed.

Figure 8b,c shows polarized absorption spectra of crystals of oxyhemoglobin and methemoglobin azide, respectively. For these derivatives, the dichroic ratios vary more with wavelength than in the case of methemoglobin crystals; however also in these derivatives, the dichroic ratio is almost uniformly greater than 1.0, consistent with the idea that the absorption is mainly due to π–π^* excitation. In the methemoglobin azide crystals, the 572-mμ shoulder in the absorption spectrum appears relatively more pronounced when the incident light is polarized perpendicular, rather than parallel to *b*. In the same crystals there also appears to be a weak absorption band (620 mμ) polarized perpendicular to *b*.

Figure 9 shows the polarized absorption spectra of chicken Hb–DNA fibers. Fiber absorbance does not significantly depend on the direction of polarization of the incident light. The visible spectra of the Hb–DNA fibers are indistinguishable from spectra of the pure Hb derivatives in solution. Since the spectrum of Hb is affected by large changes in folding of the polypeptide chains (Jope, 1949; Kaziro and Tsushima, 1959), it may be concluded that there is no gross denaturation of Hb molecules upon combination with DNA.

Polarized Visible Spectra of Cytochrome c–DNA Fibers. Crystals of oxidized and reduced horse heart Cy *c* are not isomorphous (Margoliash and Schejter, 1966); accordingly, reduction of the iron causes disruption of the ferricytochrome *c* crystals.

Figure 10 shows the polarized visible spectrum of ferricytochrome *c* crystals for light shone through the [100] or [010] planes. The dichroic ratio varies with the wavelength (2.0 at 570 mμ, and 1.2 at 530 mμ), the shoulder in the absorption spectrum at 555 mμ being most pronounced when the electric vector is polarized parallel to *c*.

Figure 11 shows the polarized visible spectra of horse heart Cy *c*–DNA fibers. The absorbance of these fibers depends significantly on the direction of polarization of the incident light. In the case of both the oxidized and reduced Cy *c* derivatives, the dichroic ratio is greater than 1.0, suggesting that the heme normals tend to lie perpendicular to the nucleoprotein fiber axis.

The shape of the visible spectra of the Cy *c*–DNA fibers are not significantly different from spectra of the pure Cy *c* derivatives in solution. Since the Cy *c* spectrum is affected by changes of configuration of the polypeptide chain (Kaziro and Tsushima, 1961), this result indicates that the protein structure is not grossly altered upon binding to DNA. Concordantly, although ferrocytochrome *c* molecules undergo spontaneous oxidation when slightly denatured (Margoliash and Schejter, 1966), it was observed that ferrocytochrome

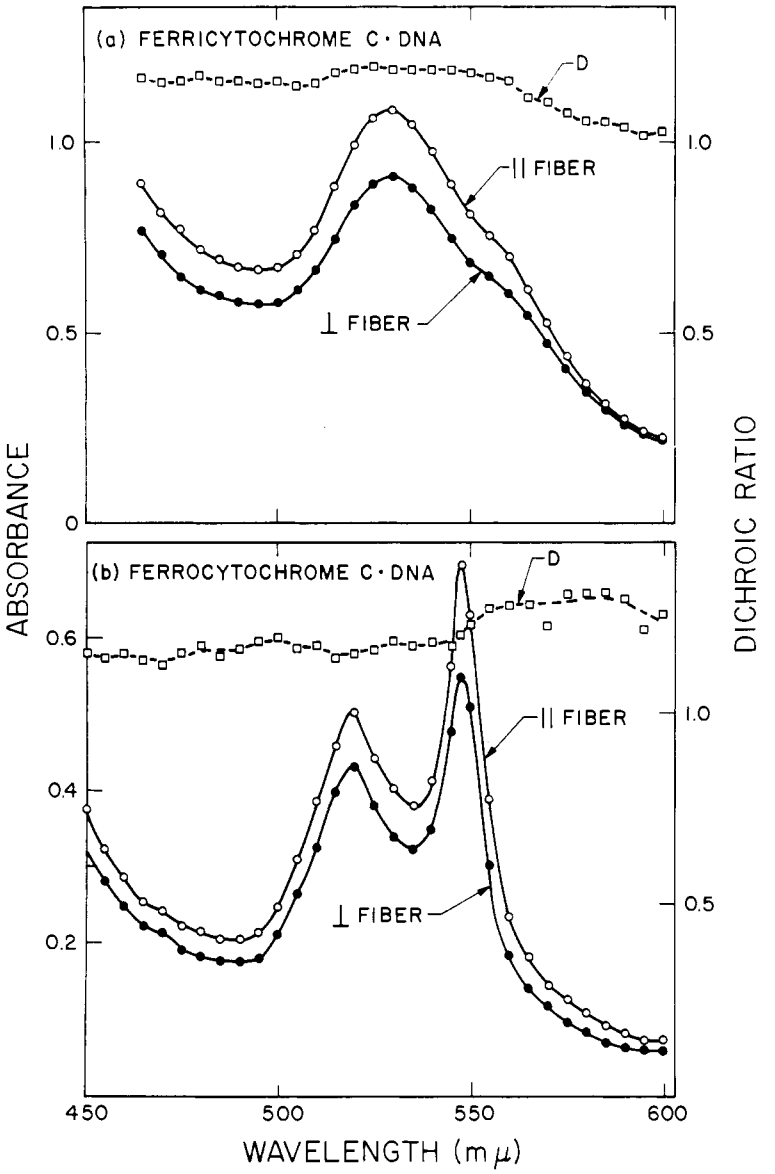

FIGURE 11: Polarized absorption spectra of horse heart Cy *c*-DNA fibers. The 550-mμ band of the ferrocytochrome *c* spectrum is extremely narrow (Margoliash and Frohwirt, 1959), and consequently absorbance here is very sensitive to spectral band width of the spectrophotometer. (a) Ferricytochrome *c*–DNA and (b) ferrocytochrome *c*–DNA. (–o–o–) Electric vector parallel to fiber axis. (–●–●–) Electric vector perpendicular to fiber axis. (– – –□– – –□– – –) Dichroic ratio.

c molecules bound into nucleoprotein fibers do not undergo spontaneous oxidation when placed in solutions exposed to air.

Discussion

Polarized Absorption Spectra of the Protein Crystals and Nucleoprotein Fibers. The hemoproteins and other porphyrin compounds all have similar visible spectra, suggesting that the absorption bands result from similar electron excitations (Falk and Perrin, 1959; Platt, 1956). It has been clearly shown, in fact, that the absorption spectrum of the porphyrins between 470 and 600 mμ is due to a pair of approximately degenerate (*i.e.*, equal energy) and perpendicularly polarized electronic transitions of the π–π^* class, each being split due to the several vibrational levels of the excited molecules (these associated vibronic bands are termed the 0–0, 0–1, etc., in order of their increasing energy) (Platt, 1956; Williams, 1956). The transition moments for such absorption are polarized in the porphyrin plane.

These two electronic transitions will be strictly degenerate only if the porphyrin has square symmetry, all four pyrrole rings being electronically equivalent

TABLE II: Estimates of Angles between Heme Normals and the Principal Axes of Refraction.

Material	Expected Dichroism for Ideal Absorber[a]	Definition of Angle θ	Obsd Av D 470–600 mμ	Calcd θ (deg)	Actual θ (deg)
Horse Met-Hb crystals	$D = \tan^2 \theta$	Between heme normal and b axis	2.1	56	58 for α heme and 57 for β heme[b]
Horse Oxy-Hb crystals			1.9	54	
Horse Met-Hb azide crystals			1.5	51	
Chicken Hb–DNA fibers (Met-Hb,Oxy-Hb, and Met-Hb azide)	No simple relationship		1.0[c]		
Horse heart ferri-Cy c crystals	$D = \frac{2 \sin^2 \theta}{1 + \cos^2 \theta}$	Between heme normal and c axis	1.4–1.6	65–70	70[d]
Horse heart Cy c–DNA fibers (ferri-Cy c and ferro-Cy c)	$D = \frac{2 \sin^2 \theta}{1 + \cos^2 \theta}$	Between heme normal and fiber axis	1.2	60	Unknown

[a] The method of obtaining these equations is described in Materials and Methods. Assumptions made in the deviations are described in the text. [b] Heme orientation in the horse hemoglobin crystals based on Ingram *et al.* (1956). [c] The absorbance of Hb–DNA fibers is independent of the polarization directions. No unique interpretation of this is possible, as the result might reflect random orientation of Hb molecules, unique orientation such that the transition moments lie on the average at 45° with respect to the fiber axis, or even several stable orientations with cancelling dichroism. [d] Heme orientation in the ferricytochrome c crystals is based on recent X-ray diffraction studies by Dickerson *et al.* (1967). Independently of the work described here, Eaton and Hochstrasser (1967) recently obtained polarized absorption spectra of Cy c crystals in close agreement with the data described here and estimated the angle as 72 ± 3°.

(Platt, 1956). Clearly, if these transitions are not degenerate, then the dichroic ratio can be expected to vary with the wavelength, the spectrum being anisotropic in the porphyrin plane. It is known that porphyrin compounds can be rendered asymmetric by substitution of side chains (*e.g.*, vinyl groups) onto the porphyrin ring; asymmetry can also be introduced as a consequence of double bonding between d orbitals of the metal and π orbitals of the tetrapyrrole (Williams, 1956; Orgel, 1959). This latter type of interaction is known to depend greatly on the oxidation state of the metal and also on the other ligands (*e.g.*, O_2, H_2O, CN^-, or imidazole) attached to the metal (Williams, 1956; Orgel, 1959). Of the different hemoprotein crystals examined, horse methemoglobin crystals (Figure 8a) are exceptional in that the dichroic ratio between 470 and 600 mμ is nearly constant, as was previously shown by Perutz (1939). Presumably, in this protein the electronic distribution in the tetrapyrrole rings is more symmetrical than in the other hemoglobin derivatives, possibly due to the relatively weak double bonding between the iron and the porphyrin as suggested by paramagnetic resonance studies (Orgel, 1959). In the other hemoproteins examined, however, the variation of D between 470 and 600 mμ suggests that the electronic transitions involved are not strictly degenerate.

As mentioned previously (Materials and Methods), when these transitions are degenerate then the heme group can be expected to act as an "ideal two-dimensional absorber" and the absorption dichroism will closely agree with the equations described. In cases of derivatives for which D varies with wavelengths, the equations given can be expected to provide only approximate estimates of the orientations of the heme groups. Table II presents calculated estimates of the orientations of heme groups in the different materials studied, as based on the observed dichroic ratios and on the dichroism expected for ideal two-dimensional absorbers. It is of interest that the estimated angles agree fairly well with the actual angles for the different derivatives of the horse hemoglobin crystals and for the ferricytochrome c crystals.

In the chicken Hb–DNA and horse heart Cy c–DNA fibers, the results indicate that the DNA molecules are aligned approximately parallel to the fiber axes. Since the protein molecules interact with DNA, their orientation in the fibers is likely to reflect the symmetry properties and orientation of the DNA. In Figure 12

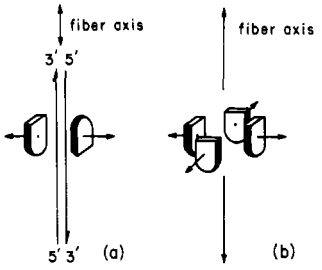

FIGURE 12: Likely degeneracies in the orientations of protein molecules with respect to a DNA fiber axis as based on the known symmetry properties of DNA (Langridge *et al.*, 1960; Langridge, 1963). (a) A 180° rotation around the axis perpendicular to fiber due to antiparallel orientation of the two strands composing the DNA double helix. (b) Rotational freedom around the fiber axis due to the helical nature of the DNA molecules. The structures with arrows represent protein molecules having DNA binding sites on the face opposite the arrow. A chromophoric prosthetic group might conceivably have any orientation with respect to the DNA binding site under consideration. In a it is assumed that the fibers have no polarity. In b it is assumed that the fibers are isotropic in cross section.

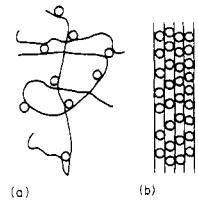

FIGURE 13: Possible function of divalent metal ions in tightly packed nucleoprotein structures. (a) Absence of Mg^{2+}, Ca^{2+}, or Mn^{2+}. Turbidity develops, but no fibers form. Probably some DNA chains are cross-linked by protein, but interchain electrostatic repulsion prevents tight packing of chains. (b) Presence of Mg^{2+}, Ca^{2+}, or Mn^{2+}. The ions bind to the nucleic acid phosphates, thereby reducing interchain electrostatic repulsion. Maximum cross-linking of DNA results in fiber formation. (The fiber structure has more cross-links per length of DNA than any other simple structure.) Protein molecules are cooperatively bound into the nucleoprotein structure. The illustrations refer to Hb–DNA fiber formation (see Results). The circles represent Hb molecules and the lines represent double-helical DNA molecules. However the basic model may be relevant to other nucleoproteins (see text).

are depicted some equally favorable protein orientations with respect to the fiber axis as based on the symmetry of DNA. The type of position degeneracy shown in Figure 12a can have no effect on the light absorption by a chromophoric protein (rotation of such a protein by 180° around an axis perpendicular to the fiber will not alter the angle between a transition moment and the fiber axis). However the type of position degeneracy shown in Figure 12b (making the fiber axis a rotational axis of symmetry) would strongly influence the light-absorbing properties of the fibers. In the calculations presented in Table II, it is assumed that such position degeneracy exists in the nucleoprotein fibers. It should be recognized, however, that protein orientation in the fibers might also be strongly influenced by protein–protein interactions and other factors not considered in Figure 12.

Function of Divalent Metal Ions in Tightly Packed Nucleoprotein Structures. The tightly packed Hb–DNA fibers studied here form only in the presence of divalent metal ions; in the absence of these cations, the Hb–DNA mixtures form only nonfibrous aggregates. Since the structurally related Cy *c*–DNA fibers also form only in the presence of divalent cations, it seems likely that the divalent metal ions play a common role in both of the nucleoprotein fibers. It is well known that the divalent metals used (Mg^{2+}, Ca^{2+}, and Mn^{2+}) bind strongly to nucleic acids, probably interacting with the negatively charged phosphate residues of the backbone (Shack and Bynum, 1959; Steiner and Beers, 1961; Dove and Davidson, 1962; Felsenfeld and Huang, 1959; Felsenfeld and Rich, 1957; Katchalsky, 1964). This suggests that the divalent metal ions might act by virtue of their binding to the nucleic acids rather than to the protein moieties.

Figure 13 shows a model of the divalent cation-induced formation of Hb–DNA fibers. This model contains the following basic ideas. (1) Electrostatic repulsion in the absence of divalent cations inhibits close association and tight packing of DNA chains (a "DNA chain" is considered to be a double-helical segment of a DNA molecule; association between DNA chains might therefore be either inter- or intramolecular). (2) Hb molecules have at least two "sites" able to interact with, and thereby to cross-link, adjacent DNA chains. The noncovalent cross-linking of DNA chains is favored when interchain electrostatic repulsion is reduced by divalent cation addition. (3) Parallel DNA orientation and fiber formation is a natural consequence of the cross-linking of DNA chains, the parallel arrangement allowing more cross-links per length of DNA than any other simple structure.

In the model shown in Figure 13, the protein molecules cooperatively hold adjacent DNA chains in a favorable binding position; this is consistent with the experimentally observed cooperative binding of Hb molecules to the fibers. A bidentate ligand (in this case a ligand having two binding sites for DNA) would be expected to bind many times more strongly to the fibers (where both sites could simultaneously interact with DNA chains) than to DNA molecules in solution (where presumably only one site could interact with DNA). Therefore, the binding of such ligands to DNA should be weakened in conditions where extensive cross-linking is prevented (*e.g.*, in the absence of divalent metal ions); this might explain the increased

level of Hb binding which initially accompanies the divalent cation-induced fiber formation. The decline of Hb:DNA ratio as the $MgCl_2$ concentration is further raised (Figure 2) could be due to various secondary effects such as competition between the Mg^{2+} and Hb for sites on the DNA. The dyad symmetry and subunit structure of Hb (Perutz, 1965) is consistent with the requirement that this protein must have at least two binding sites. Furthermore, the existence of strong electrostatic repulsion between DNA chains in low ionic strength media in the absence of divalent cations, even when the chains are separated by 50 A (the approximate diameter of a Hb molecule), is consistent with theoretical studies concerning electrostatic fields surrounding cylindrical polyions (Katchalsky, 1964).

A second model by which the effects of the divalent cations might be explained is that these ions themselves form bridges between adjacent DNA chains, thereby causing nucleoprotein aggregation. This latter explanation is unlikely for several reasons. In the first place, this model explains neither the role of the protein nor the cooperative binding of the protein molecules into the fibers. In the absence of protein, it may be noted that divalent cations (Ca^{2+}, Mg^{2+}, or Mn^{2+}) do not precipitate DNA. In addition, from the composition of typical hydrated Hb–DNA fibers used in this study (DNA:protein:H_2O present in the mass ratio 1:3.4:2.1), it can be calculated that the average distance between adjacent DNA chains is roughly 46 A (*i.e.*, approximately 30 A between the outer surfaces of the two adjacent chains); therefore, metal ion bridges, if they exist, could only occur infrequently between adjacent nucleic acid chains.

One major feature of the model shown in Figure 13 is the concept that the divalent metal ions influence the Hb–DNA interaction as a result of their binding to the nucleic acid rather than to the protein moieties. This suggests that other proteins having at least two binding sites might also cross-link nucleic acid chains most readily in the presence of at least low levels of divalent cations. That the role of divalent metal ions as elaborated in Figure 13 is indeed not unique to the Hb–DNA interaction, and may in fact be relevant to many nucleoproteins, is consistent with the information below.

(i) Treatment of animal or plant cell chromosomes in low ionic strength solutions causes nucleoprotein swelling only if the divalent metal ion concentration is very low (*e.g.*, less than about 5×10^{-4} M $MgCl_2$). This has been reported in a wide variety of systems including *Drosophila melanogaster* salivary glands and mitotic and meiotic cells from grasshopper testis (Mazia, 1954), chicken erythrocytes (Davies and Spencer, 1962), *Vicia faba* root cells (Hyde, 1956), isolated metaphase chromosomes from mouse leukemia cells, Chinese hamster cells, and HeLa cells (Chorazy *et al.*, 1963; Somers *et al.*, 1963; J. A. Huberman, personal communication), and sea urchin sperms (Mazia, 1954; Solari, 1965). In all cases the native condensed morphology of the chromosome appears to depend critically upon the divalent cation concentration.

Soluble chromatin or nucleohistone can only be obtained by shearing chromosomes in the swollen state (*i.e.*, in low ionic strength solutions in the absence of divalent cations) (Zubay and Doty, 1959; Marushige and Bonner, 1966); the soluble chromatin so obtained is precipitated by low levels (*ca.* 0.001–0.002 M $MgCl_2$), of divalent metal ions (Bonner and Huang, 1966; Sonnenberg and Zubay, 1965). X-Ray diffraction studies of intact nuclei from chicken erythrocytes and calf thymocytes suggested a model of *in vivo* chromosomes in which *histone bridges* cross-link parallel-oriented DNA chains into a large three-dimensional aggregate (Wilkins, 1959; Wilkins *et al.*, 1959). That the histone bridges are labile and are broken in low ionic strength media as a consequence of electrostatic repulsion between DNA chains was suggested by Wilkins (1959). Histone cross-linking of parallel-oriented chromosomal DNA chains was also suggested by Luzzatti and Nicolaieff (1959) on the basis of their X-ray diffraction studies.

Studies of heterochromatin and euchromatin (Littau *et al.*, 1964) and of "puffing" in dipteran salivary gland chromosomes (Kroeger and Lezzi, 1966) suggest that the tightness of packing of chromosomal DNA chains might be an important factor in the regulation of genetic activity. If the difference between tightly packed and swollen chromatin is indeed a matter of histone cross-linking, then the factors regulating such cross-linking are of obvious biological importance. According to the model shown in Figure 13, one factor of importance in the heterochromatin to euchromatin transition might be the electrostatic repulsion between adjacent DNA chains; such electrostatic repulsion might be increased in a chromosomal region by removal of metal ions from the DNA, by removal of histones from the DNA, or by addition of polyanions to the DNA. The cooperative nature of the protein cross-linking of nucleic acid chains (Figure 13) leads to the expectation that neighboring histone cross-links would tend to break synchronously, giving rise to a localized "melting" phenomenon; consequently, small changes in the environment might induce large changes of chromosomal structure.

(ii) It is well known that magnesium ions are necessary for the structural integrity of ribosomal particles (Goldberg, 1966; Gavrilova *et al.*, 1966). Furthermore, X-ray diffraction studies (Langridge, 1963) have suggested that the ribonucleic acid chains of ribosomes may be arranged in the form of several parallel-oriented-double helices.

As compared with divalent metal ions, monovalent cations (*e.g.*, Na^+, K^+, and NH_4^+) exert only a relatively weak influence not only on the nucleoprotein structures discussed here, but also on many reactions of nucleic acids, including thermal denaturation of double-stranded nucleic acids (Dove and Davidson, 1962; Felsenfeld and Rich, 1957) and binding of some cationic dyes to nucleic acid phosphates (Waring, 1965; Steiner and Beers, 1961). Such monovalent cations probably do not strongly bind onto the phosphates, but rather form a relatively loose atmosphere of counterions in the surrounding solution (Katchalsky,

1964). Therefore, if two nucleic acid chains were packed together such that very little solution were *interposed* between them (either by very close association or by having a larger interchain space completely occupied by protein), then the concentration of monovalent salt in the *surrounding* solution would be expected to have little influence on the electrostatic repulsion between the chains. In such a case, divalent metal ions might exert a primary influence on the stability of protein cross-links even at relatively high concentrations of monovalent salts.

Acknowledgments

I wish to thank Drs. G. Attardi, D. Robberson, and P. Callis for helpful discussions. I am grateful to Dr. R. E. Dickerson for the generous gift of cytochrome *c* crystals, to Drs. K. Zankel, P. Burke, and M. Delbrück for help with their microspectrophotometer, and to LaVerne Wenzel for her assistance.

References

Bonner, J., and Huang, R. C. (1966), *Biochem. Biophys. Res. Commun. 22*, 211.

Burgi, E., and Hershey, A. D. (1963), *Biophys. J. 3*, 309.

Chorazy, M., Bendich, A., Borenfreund, E., and Hutchinson, D. J. (1963), *J. Cell Biol. 19*, 59.

Cole, A. (1957), *in* Theoretical and Experimental Biophysics, Vol. 1, Cole, A., Ed., New York, N. Y., Marcel, p 305.

Davies, H. G., and Spencer, M. (1962), *J. Cell Biol. 14*, 445.

Dickerson, R. E., Kopka, M. L., Weinzierl, J., Varnum, J., Eisenberg, D., and Margoliash, E. (1967), *J. Biol. Chem. 242*, 3015.

Doty, P., McGill, B. B., and Rice, S. A. (1958), *Proc. Natl. Acad. Sci. U. S. 44*, 432.

Dove, W. F., and Davidson, N. (1962), *J. Mol. Biol. 5*, 467.

Eaton, W. A., and Hochstrasser, R. M. (1967), *J. Chem. Phys.* (in press).

Falk, J. E., and Perrin, D. D. (1959), *in* Haematin Enzymes, Falk, J. E., Lemberg, R., and Morton, R. K., Ed., London, Pergamon, p 56.

Felsenfeld, G., and Huang, S. (1959), *Biochim. Biophys. Acta 34*, 234.

Felsenfeld, G., and Rich, A. (1957), *Biochim. Biophys. Acta 26*, 457.

Gavrilova, L. P., Ivanov, D. A., and Spirin, A. S. (1966), *J. Mol. Biol. 16*, 473.

Goldberg, A. (1966), *J. Mol. Biol. 15*, 663.

Hashimoto, K., and Wilt, F. H. (1966), *Proc. Natl. Acad. Sci. U. S. 56*, 1477.

Huisman, T. H. J., and Prins, H. K. (1955), *J. Lab. Clin. Med. 46*, 255.

Huisman, T. H. J., Schillhorn Van Veen, J. M., Dozy, A. M., and Nechtman, C. M. (1964), *Biochim. Biophys. Acta 88*, 352.

Hyde, B. B. (1956), *Genetics 41*, 648.

Ingram, D. J. E., Gibson, J. F., and Perutz, M. F. (1956), *Nature 178*, 906.

Inoue, S., and Sato, H. (1962), *Science 136*, 1122.

Jope, E. M. (1949), *in* Haemoglobin, Roughton, F. J. W., and Kendrew, J. C., Ed., London, Butterworth, p 205.

Katchalsky, A. (1964), *Biophys. J. 4*, 9.

Kaziro, K., and Tsushima, T. (1959), *in* Haematin Enzymes, Falk, J. E., Lemberg, R., and Morton, R. K., Ed., London, Pergamon, p 80.

Kroeger, H., and Lezzi, M. (1966), *Ann. Rev. Entomol. 11*, 1.

Langridge, R. (1963), *Science 140*, 1000.

Langridge, R., Marvin, D. A., Seeds, W. E., Wilson, H. R., Hooper, C. W., Wilkins, M. H. F., and Hamilton, L. D. (1960), *J. Mol. Biol. 2*, 38.

Littau, V. C., Allfrey, V. G., Frenster, J. H., and Mirsky, A. E. (1964), *Proc. Natl. Acad Sci. U. S. 52*, 93.

Luzatti, V., and Nicolaieff, A. (1959), *J. Mol. Biol. 1*, 127.

Maestre, M. F., and Kilkson, R. (1965), *Biophys. J. 5*, 275.

Manwell, C., Baker, C. M. A., Roslansky, J. D., and Foght, F. (1963), *Proc. Natl. Acad. Sci. U. S. 49*, 496.

Margoliash, E., and Frohwirt, N. (1959), *Biochem. J. 71*, 570.

Margoliash, E., and Schejter, A. (1966), *Advan. Protein Chem. 21*, 113.

Marushige, K., and Bonner, J. (1966), *J. Mol. Biol. 15*, 160.

Matsuda, G., and Takei, H. (1963), *J. Biochem. 54*, 156.

Mazia, D. (1954), *Proc. Natl. Acad. Sci. U. S. 40*, 521.

Murayama, M., Olson, R. A., and Jennings, W. H. (1965), *Biochim. Biophys. Acta 94*, 194.

Olivera, B. (1966), Ph.D. Thesis, California Institute of Technology, Pasadena, Calif.

Orgel, L. E. (1959), *in* Haematin Enzymes, Falk, J. E., Lemberg, R., and Morton, R. K., Ed., London, Pergamon, p 1.

Pattri, H. O. E. (1932), *Z. Zellforsch. 16*, 723.

Perutz, M. F. (1939), *Nature 143*, 731.

Perutz, M. F. (1947), *Proc. Roy. Soc. (London) A191*, 83.

Perutz, M. F. (1965), *J. Mol. Biol. 13*, 646.

Perutz, M. F., and Mitchison, J. M. (1950), *Nature 166*, 677.

Platt, J. R. (1956), *in* Radiation Biology III, Hollaender, A., Ed., New York, N. Y., McGraw-Hill, p 71.

Saha, A. (1964), *Biochim. Biophys. Acta 93*, 573.

Shack, J., and Bynum, B. S. (1959), *Nature 184*, 635.

Solari, A. J. (1965), *Proc. Natl. Acad. Sci. U. S. 53*, 503.

Somers, C. E., Cole, A., and Hsu, T. C. (1963), *Exptl. Cell Res., Suppl. 9*, 220.

Sonnenberg, B. P., and Zubay, G. (1965), *Proc. Natl. Acad. Sci. U. S. 54*, 415.

Steiner, R. F., and Beers, R. F., Jr. (1961), Poly-

nucleotides, Amsterdam, Elsevier, p 290.
Stewart, R. F., and Davidson, N. (1963), *J. Chem. Phys. 39*, 255.
Stoves, J. L. (1957), Fibre Microscopy, London, National Trade, p 61.
Van der Helm, H. J., and Huisman, T. H. J. (1958), *Science 127*, 762.
Waring, M. J. (1965), *J. Mol. Biol. 13*, 269.
Wilkins, M. H. F. (1959), *in* Nucleoproteins, Stoops, R., Ed., New York, N. Y., Interscience, p 45.
Wilkins, M. H. F., Zubay, G., and Wilson, H. R. (1959), *J. Mol. Biol. 1*, 179.
Williams, R. J. P. (1956), *Chem. Rev. 56*, 299.
Wood, E. A. (1964), Crystals and Light, Princeton, N. J., D. Van Nostrand.
Zubay, G., and Doty, P. (1959), *J. Mol. Biol. 1*, 1.

Synthesis of [5-Isoleucine,8-alanine]-angiotensin II by the Solution Method Synthesis and the Solid-Phase Method Synthesis*

Won Kil Park, Robert R. Smeby, and F. Merlin Bumpus

ABSTRACT: The octapeptide [5-isoleucine,8-alanine]-angiotensin II has been synthesized using a solution synthetic method and a solid-phase method of synthesis. With both methods, the final product was chromatographically homogeneous and gave the correct amino acid analysis and identical biological activity. The solid-phase method of peptide synthesis gave the final product in much greater speed and in higher yield. [5-Isoleucine,8-alanine]-angiotensin II possesses about 1% of the pressor activity of [5-isoleucine]-angiotensin II, indicating the great importance of the aromatic group in position 8 of the natural peptide.

From studies on numerous analogs of angiotensin II, the phenolic ring of tyrosine (Page and Bumpus, 1961; Seu *et al.*, 1962b), the imidazole ring of histidine (Paiva and Paiva, 1961; Page and Bumpus, 1961), the pyrolidine ring of proline (Seu *et al.*, 1962a; Sivanandaiah *et al.*, 1966), and the C-terminal carboxyl group are all required for the compound to exhibit biological activity. The side groups of the amino acids aspartic acid and arginine can be modified greatly with minimal effects on the biological properties of the peptide (Page and Bumpus, 1961; Havinga *et al.*, 1964; Arakawa and Bumpus, 1960; Brunner and Regoli, 1962). It therefore seemed of considerable interest to determine the importance of the aromatic ring (Page and Bumpus, 1961; Sivanandaiah *et al.*, 1966) of the C-terminal phenylalanine for biological activity. For this reason [5-isoleucine,8-alanine]-angiotensin II[1] was prepared in which the aromatic ring of phenylalanine has been eliminated by both solution method of synthesis and the solid-phase method as reported by Merrifield (1963) and Marshall and Merrifield (1965).

Results and Discussion

The outline of the method used for synthesis of this peptide in solution is given in Figure 1. The carboxyl group of the C-terminal alanine was blocked as the *p*-nitrobenzyl ester. Carbobenzoxyproline was condensed with alanine *p*-nitrobenzyl ester by the mixed-anhydride procedure to yield carbobenzoxyprolylalanine *p*-nitrobenyzl ester in 92% over-all yield. Carbobenzoxyisoleucine was coupled with *N*-(imidazolebenzyl)histidine methyl ester using DCCI as a condensin gagent to give carbobenzoxyisoleucyl(imidazolebenzyl)histidine methyl ester in 70% yield. This methyl ester converted to carbobenzoxyisoleucyl(imidazolebenzyl)histidine hydrazide which was condensed by the azide procedure with prolylalanine *p*-nitrobenzyl ester to yield the blocked tetrapeptide. After removal of the carbobenzoxy group of this tetrapeptide with HBr in acetic acid, it was condensed with carbobenzoxyvalyltyrosine azide to yield the hexpeptide carbobenzoxyvalyltyrosylisoleucyl(imidazolebenzyl)histidylprolylalanine *p*-nitrobenzyl ester in 43% yield. The carbobenzoxy group was again removed with HBr in acetic acid and the free-base hexapeptide was obtained by treating the product with 1 M potassium bicarbonate. The blocked octapeptide was obtained

* From the Research Division, Cleveland Clinic Foundation, Cleveland, Ohio 44106. *Received June 23, 1967.* This work was partially supported by U. S. Public Health Grant 6835.

[1] All amino acids are the L isomer. Abbreviations used: Z, carbobenzoxy; Boc, *t*-butoxycarbonyl; DCCI, dicyclohexylcarbodiimide.